THESIS FOR THE DEGREE OF LICENTIATE OF ENGINEERING

Model-Based Optimization of Hydronic Heating System Operations

Enhancing Comfort and Energy Efficiency in the Existing Building Stock

Henrik Håkansson

Department of Electrical Engineering
Chalmers University of Technology
Gothenburg, Sweden, 2025

Model-Based Optimization of Hydronic Heating System Operations

Enhancing Comfort and Energy Efficiency in the Existing Building Stock

Henrik Håkansson

Department of Electrical Engineering
Chalmers University of Technology
SE-412 96 Gothenburg, Sweden
Phone: +46 (0)31 772 1000

Printed by Chalmers Digital Printing
Gothenburg, Sweden, October 2025

Model-Based Optimization of Hydronic Heating System Operations

Enhancing Comfort and Energy Efficiency in the Existing Building Stock

Henrik Håkansson
Department of Electrical Engineering
Chalmers University of Technology

Abstract

Space heating accounts for 30% of the total energy use in the EU, and to reduce costs and meet climate goals, efficient operation that maintains comfort must be developed. Hydronic heating is popular and attractive, as it is compatible with efficient heat production and distribution. The operation of hydronic systems typically provides good comfort, but high peak loads and overheating are common, particularly in older, poorly insulated buildings.

Recent deployments of sensors have improved dynamic control of the supply temperature via air temperature feedback, as used in model predictive control (MPC). Although this has led to reduced overheating, static configurations still limit performance. This thesis explores modeling of building thermal dynamics to improve two such configurations—district heating price models and flow rate balancing—enabling cheaper and more efficient operation.

District heating price models incentivize desirable operation of hydronic systems, and with cost-optimizing control (economic MPC), these incentives have an immediate effect. While price models often target total energy consumption, limiting peak loads also benefits district heating companies. Penalizing peak demand encourages shifting loads in time by exploiting building thermal inertia. By simulating optimal control, we show that strong peak-demand penalties can reduce overall peak load in a district heating network by 10–20% compared to models without such incentives.

Within a hydronic system, all radiators share a centrally controlled supply temperature. To ensure uniform temperatures and heat supply across zones, flow rates must be balanced through statically configured valves. The effect of adjusting those valves is often not obvious, as the zonal temperature variations depend on the weather. With a thermal dynamics model, we show how zonal variations relate to the angle between two parameter vectors. Using operational data, we demonstrate weather-independent evaluation of balancing by comparing this angle before and after adjustments.

The proposed methods are compatible with existing equipment, enabling immediate real-world implementation.

Keywords: Hydronic heating, dynamic modeling, optimal control, hydronic balancing, load shifting

List of Publications

This thesis is based on the following publications:

[A] **Henrik Håkanson**, Magnus Önnheim, Emil Gustavsson, Mats Jirstrand, "Effects on District Heating Networks by Introducing Demand-Side Economic Model Predictive Control". Published in Energy & Buildings 309.

[B] **Henrik Håkanson**, Magnus Önnheim, Jonas Sjöberg, Mats Jirstrand, "Model-Assisted Hydronic Balancing in Residential Heating Systems using Operational Sensor Data". Accepted in Energy & Buildings.

Other publications by the author, not included in this thesis, are:

[C] **Henrik Håkansson**, Magnus Önnheim, Jonas Sjöberg, Mats Jirstrand, "A data-driven model-based approach for balancing hydronic heating systems in residential buildings". European Research Network System Identification (ERNSI) Workshop, Venice, Italy, 21-24 September 2024, Abstract No. 2.16.

[D] **Henrik Håkansson**, Magnus Önnheim, Emil Gustavsson, Mats Jirstrand, "Effects from large-scale employment of model-predictive control in district heating substations". Kaiserslautern Applied and Industrial Mathematics Days (KLAIM2023), 25 - 27 September 2023, Abstract No. A20, p.33.

[E] **Henrik Håkansson**, Anders Sjöberg, Maria Carmen Toribio, Magnus Önnheim, Michael Olberg, Emil Gustavsson, Michael Lindqvist, Mats Jirstrand, John Conway, "Utilization of Convolutional Neural Networks for H I Source Finding: Team FORSKA-Sweden approach to SKA Data Challenge 2". Astronomy & Astrophysics, Vol 671, March 2023, A39.

[F] **Henrik Håkansson**, Magnus Önnheim, Emil Gustavsson, Mats Jirstrand, "Model predictive control for heating systems when using demand tariffs". Smart Energy Systems 2022, Aalborg. September 13-14 2022.

[G] **Henrik Håkansson**, Anders Sjöberg, Maria Carmen Toribio, Magnus Önnheim, Michael Olberg, Emil Gustavsson, Michael Lindqvist, Mats Jirstrand, John Conway, "Utilization of Convolutional Neural Networks for H I Source Finding: Team FORSKA-Sweden approach to SKA Data Challenge 2". European Astronomical Society Annual Meeting 2022. Valencia, Spain, 27 June-1 July, 2022.

Contents

Acknowledgments

This work is the result of a collaboration between the Fraunhofer-Chalmers Centre for Industrial Mathematics (FCC) and the Department of Electrical Engineering at Chalmers University of Technology. It has been financially supported by the Swedish Foundation for Strategic Research (SSF).

The research was further enabled through the valuable collaboration with the municipal housing company Örebrobostäder. I am grateful to Jonas Tannerstad for generously providing operational data and supporting the research, and especially to Pedram Zadeh at Örebrobostäder for patiently sharing your expertise in hydronic balancing and for your openness to experimentation and innovation.

I am thankful to my supervisors, Mats Jirstrand, Magnus Önnheim, and Jonas Sjöberg, for their invaluable guidance throughout this work. Your thoughtful feedback, especially on clarity and pedagogy, has helped shape the direction and quality of the research. I also thank co-authors Anders Sjöberg and Emil Gustavsson for insightful discussions and support during the writing process.

A warm thank you to all my colleagues at FCC. In particular, I appreciate those of you who shared many lunches and conversations with me in the large lunchroom on the fourth floor—it made the everyday work all the more enjoyable.

Finally, my deepest gratitude goes to Aina. Thank you for your love and support, through both headwinds and tailwinds.

Part I

Overview

CHAPTER 1

Background

1.1 Introduction

Transforming energy utilization from wasteful and unaware to efficient and clever has rarely been more relevant than today. To reach the long-term goal of climate neutrality, which the European Union (EU) aims for in 2050 [1], energy efficiency is arguably crucial to enable fully sustainable solutions. However, in 2022, when Russia invaded Ukraine and through the widespread energy crisis that followed, it became clear that streamlining energy usage is an urgent matter here and now. Since then, energy issues have become extraordinarily relevant to financial and security concerns, reminiscent of the 1973 oil crisis. Two winters in a row, the EU members have agreed to drastically reduce the gas demand by 15% [2], [3]. Together with peaking energy prices, these actions have had a particular impact on the European heating sector [4], and room temperatures have reportedly been decreased [5]. While those measures may have mitigated the situation in the short term, they were never desired by the users and will not form any definitive solution to the underlying problems.

Given these challenges, the development and deployment of heating systems that can sustainably deliver thermal comfort is crucial for achieving

more efficient and resilient energy use. Hydronic systems — centrally heated, water-based heating solutions [6] — are well-suited to this transition due to their compatibility with high-efficiency heat sources such as heat pumps [7], [8] and district heating networks [9]. In Sweden, hydronic radiator systems predominantly supplied by district heating account for the majority of heat delivery in residential and service sectors [10], [11]. While the Swedish configuration is widely regarded as both efficient and environmentally friendly — often cited as a model for other countries [12] — the sector has not been unaffected by increased operational costs, as competition for energy resources has intensified [13]. With an aging building stock that, to a large extent, remains energy-inefficient [14], [15], improved control has been highlighted as a key step for further progress [16].

In a Swedish context, heat transfer from the district heating network to the hydronic system is primarily regulated by controlling the supply temperature at the building's substation [17]. An excessive supply temperature causes overheated thermal zones and leads to unnecessary energy consumption [18]. Conversely, too low a supply temperature can result in underheated zones and discomfort. In recent years, Swedish housing companies have deployed indoor air temperature sensors and remotely accessible actuators at a large scale, enabling supply temperature control with feedback from the zone temperatures [19]. These improvements in the control of the supply temperature has led to reduced overheating and more stable indoor climates, achieving better energy efficiency without compromising thermal comfort.

Despite these recent improvements, there are significant challenges yet to be solved. With the substation forming an interface between the district heating network and the hydronic system, the supply temperature control manages the inter-system energy flow, as illustrated in Figure 1.1. On the district heating side, production must meet the aggregated heat demand of many substations — but the demand is shaped by local supply temperature control decisions. To coordinate production with this demand, energy suppliers rely on pricing mechanisms that incentivize demand-side behavior consistent with cost-efficient generation [20]. Production is typically more expensive and less efficient during peak load periods [21] — such as during cold weather. However, if price models do not reflect these costs—by, e.g., penalizing high demand—even advanced supply temperature controllers that optimize operational costs have no signal to reduce peak loads for supporting system-wide

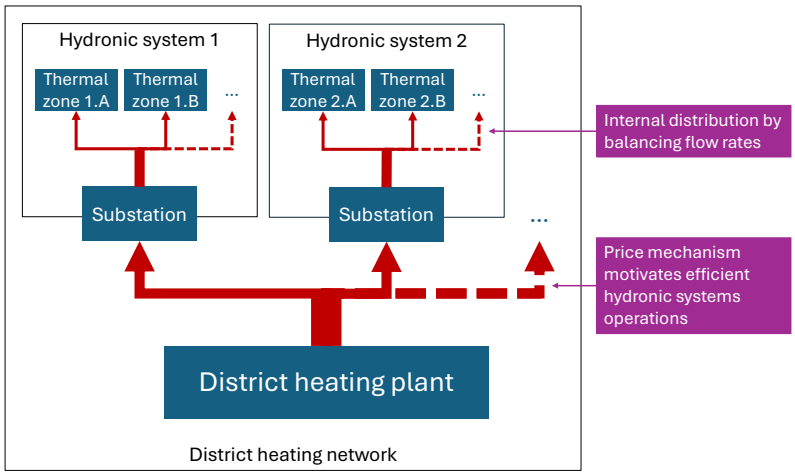

Figure 1.1: Energy flow. Conceptual map of hydronic systems in a district heating network, illustrating how energy flows through the system. Flow rate balancing influences the intra-distribution of energy between thermal zones in a hydronic system, while price mechanisms are applied at the substation level and primarily affect heating power supply over time.

efficiency.

Another challenge, not addressed by the employment of feedback control, is that, besides the supply temperature, the flow rates also affect the radiators' heat output. By *balancing* the flow rates, each radiator can output an appropriate amount of heat such that air temperatures are uniform across the building [22]. Balancing flow rates is typically achieved by manually configuring valves at various positions in the pipe network. Improper valve configuration leads to flow imbalances—some zones receive insufficient flow (underflow), while others receive excessive flow (overflow). In such scenarios, local thermostatic radiator valves (TRVs) cannot fully correct the discrepancies. Consequently, the centrally controlled supply temperature must be increased to compensate for underheated zones, which in turn overheats the zones with excess flow, resulting in significant energy waste [23].

Both in designing price mechanisms and balancing flow rates, the complexity of hydronic systems and district heating networks demands substantial expert knowledge [24]. Even experienced professionals often have to rely on trial-and-error, as predicting the effects of new price models or rebalanced flow rates remains difficult [25]. Moreover, the consequences of these interventions are not always immediately visible, as system performance depends on time-varying conditions such as outdoor temperature [26]. A new price model or flow rate balancing may seem successful after a week in mild weather, only to reveal significant shortcomings when colder conditions arrive. As a result, evaluating and refining these strategies requires long development cycles, and outcomes are often suboptimal: indoor temperatures vary across zones, and price models may fail to promote favorable demand-side behavior.

In summary, the distribution mechanisms within both the hydronic system (i.e., flow rate balancing) and the district heating network (price model design) constrain the energy efficiency and comfort performance that any supply temperature controller can achieve. This thesis investigates model-based strategies to support and accelerate the design, decision-making, and operational processes associated with these distribution mechanisms. In particular, dynamic models of the building heat dynamics are used for studying price model design and flow rate balancing. Further, a system perspective is adopted for developing mechanisms that work well together with optimal supply temperature control, striving to maximize the overall system performance.

1.2 Contributions

This thesis is based on two papers, Paper A and Paper B, each with a distinct scope, yet both centered around hydronic system operations with optimized supply temperature control.

Paper A explores price models in district heating networks, offering insights valuable to district heating suppliers aiming to leverage supply temperature controllers in the substations to improve overall system efficiency. The main contributions of this paper are:

- A simulation study demonstrating that price models incorporating peak demand penalties can incentivize load-shifting strategies, resulting in peak demand reductions of 10–20% with only a minor increase in total energy consumption (1–2%)

- Further exploration of load shifting strategies in both time and space through coordinated supply temperature control across all demand points. By avoiding simultaneous peaks in different substations, the simulations indicate an additional peak reduction potential of up to 6%.

Paper B develops modeling and methods informed by sensor data to improve hydronic balancing conditions and thereby reduce temperature variations between thermal zones and mitigate costly overheating. The main contributions of this paper are:

- The development of a method for evaluating flow rate balancing with respect to thermal comfort, independent of weather conditions and supply temperature settings. Data from a residential heating system demonstrates how a well-balanced configuration, according to the evaluation method, aligns with low temperature variation.
- A model-based framework for recommending flow rate rebalancing, informed by operational data collected from indoor air temperature sensors. Applying this to the same residential heating system data shows that the framework successfully anticipates the effect rebalancing has on the thermal conditions.

1.3 Thesis Outline

The structure of the thesis is as follows: Chapter 2 explains the relevant aspects of the operations of hydronic systems and the challenges associated with this. Chapter 3 provides an overview of modeling approaches for thermal dynamics, which form the basis of Papers A and B. Chapter 4 describes how the modeling tools can be utilized for supply temperature control and flow rate balancing. Chapter 5 gives a summary of Papers A and B. Chapter 6 provides the most important conclusions from this thesis and outlines possibilities for future work.

CHAPTER 2

Hydronic System Operations

The structure and operational practices of hydronic systems can vary depending on factors such as the system's age, regional context, and heat source. This section outlines the basic characteristics of radiator systems supplied by district heating as they typically are configured in a Swedish context. Section 2.1 describes the key components and available control mechanisms. Section 2.2 gives an overview of the desired behavior and performance goals addressed in Papers A and B. Section 2.3 explains how control mechanisms are typically implemented in current systems and how they can be leveraged to meet the performance goals.

2.1 System Components

In the hydronic system, supply water is heated in a district heating substation, pumped to radiators located in thermal zones where it deposits heat and thereby is cooled, and then returned to the substation for reheating. This section briefly reviews the main components, their functions, and the control mechanisms.

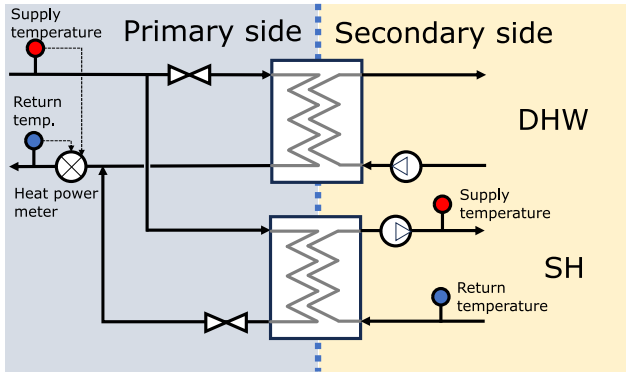

Figure 2.1: Substation structure Schematic illustrating the district heating supply used for domestic hot water (DHW) and space heating (SH) on the secondary side. It includes two heat exchangers and valves controlling the primary flow. Supply and return temperatures are measured on both sides, and total heating power is monitored by a heat meter on the primary side.

Substation

At the substation, heat from the district heating transfers to the building's hydronic system via a heat exchanger in a hydraulically separated manner [17]. The part that belongs to the district heating network is commonly referred to as the *primary side*, while the part that belongs to the hydronic system is referred to as the *secondary side*. The district heating water is also used for domestic hot water (DHW) via its heat exchanger. The water in the hydronic system, on the secondary side, is circulated by a pump mounted in the substation. A typical layout for a substation is visualized in Figure 2.1.

The district heating supplier charges the consumer—typically the housing company that owns the hydronic system and substation—based on data collected by sensors on the primary side, as illustrated in Figure 2.1, primarily through the heat power meter. The primary side's supply temperature is centrally controlled at the district heating plant and cannot be adjusted at the substation. Heat transfer from the primary to the secondary side is managed by adjusting the flow rate on either side of the heat exchanger. In Sweden, the most common variant is to maintain a relatively constant flow rate on the secondary side, while the primary side flow rate is regulated via a control valve

[17]. The opening of that valve is controlled with a setpoint for the supply temperature to the radiator system on the secondary side. By contrast, in other countries—such as Denmark—it is common to regulate heat transfer by varying the pump speed and thereby the flow rate on the secondary side. Regardless of whether the regulation is implemented on the primary or secondary side, the consumer effectively controls the total amount of heat delivered to all thermal zones.

Pipe Network

The most common distribution network structure consists of two parallel pipes: a supply pipe and a return pipe [6]. Although less common, alternative piping structures—such as single-pipe or three-pipe systems—also exist. With the two-pipe structure, the supply pipe transports heated water from the substation to the radiators, while the return pipe carries the cooled water back. Each radiator has its inlet connected to the supply pipe and its outlet to the return pipe. In multi-storey buildings, a typical layout involves main pipes in the basement from which riser pipes are branched from a main pipe, such that radiators on vertically stacked positions are supplied by the same riser, which is visualized in Figure 2.2.

At the bottom of each riser, there is typically a balancing valve, *riser valve*, used to adjust the flow rate in all radiators connected to the riser [23]. The most common type is valves that are manually configured with a static valve opening to maintain a constant hydraulic resistance [27]. These valves are equipped with measurement nipples that enable occasional flow rate measurements using an external device. However, such measurements are not performed regularly, but rather on an as-needed basis. Manually configurable balancing valves still dominate in the existing building stock [24], although valves with dynamically controlled resistance have become available recently. These devices actively measure the pressure on the supply and return pipes and adjust the resistance to maintain a constant differential pressure [28]. While automatic valves can improve system performance, they still need to be configured, and also impose higher initial investment costs [29].

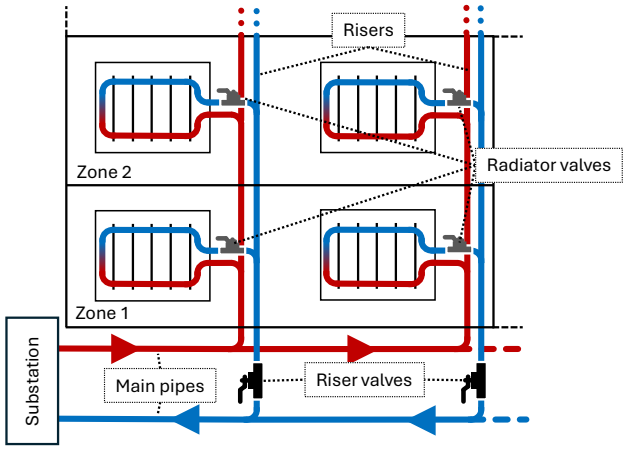

Figure 2.2: Two-pipe system Structure of a two-pipe system in a multi-storey building with risers. Riser valves are mounted on the bottom of the return pipe at each riser, while radiator valves are mounted on the return pipe from each radiator.

Radiators and Thermal Zones

In each radiator, the hot supply water is cooled to the return temperature through heat exchange with the surrounding air in the thermal zone. In a two-pipe system, all radiators receive water at the same inlet temperature—the supply temperature set centrally at the substation—while the flow rate can vary between radiators. These flow rates are configured through the riser and radiator valves, as shown in Figure 2.2.

Additionally, radiators are usually equipped with thermostatic radiator valves (TRVs), which are dynamically clamped to adjust the flow rate with feedback from the local air temperature. The most common variant is mechanical TRVs, which are based on an expansion valve mechanism [30]. Nowadays, there also exist electronic TRVs, which clamps using a stepper motor [31], although they are reportedly not common in the Swedish building stock yet [32].

While it was relatively uncommon just a few years ago [18], it is now more or less standard practice to monitor the air temperature inside the thermal

zone using a sensor mounted on the wall in the hall of each apartment [19]. Although indoor climate conditions may vary between rooms, the hallway is chosen because it serves as a representative location: ventilation design typically ensures that air from all rooms circulates through this central point, making the measured temperature a good proxy for the apartment's overall thermal condition.

2.2 Challenges and Opportunities

Housing companies are responsible for ensuring a comfortable indoor climate, while utility suppliers charge based on the amount of heat energy consumed at the substation. As a result, the operation of hydronic heating systems typically seeks to balance three interrelated objectives: indoor comfort, energy consumption, and operational cost. These objectives are tightly coupled—both comfort and cost are directly influenced by energy use. More broadly, the goal is to enable an energy-efficient heating solution overall. This section briefly outlines how these objectives present both challenges and opportunities for improvement.

Demand-Side Behavior for District Heating

District heating systems rely on various types of boilers, generally categorized into base and peak capacity units [21]. Base capacity units are cost-effective and typically use environmentally friendly fuels, such as residual waste, but are unable to respond to sudden changes in heat demand. In contrast, peak capacity units are more responsive but are often fossil-fueled and expensive. Therefore, the system's overall energy performance depends on the extent to which peak capacity is utilized.

While overall heat demand is strongly influenced by weather, several studies have demonstrated that the thermal inertia of buildings can be leveraged for load shifting—i.e., reducing peak demand by shifting heat loads to earlier or later periods [33]–[35]. Figure 2.3 illustrates such a strategy: by preheating before the coldest period, peak demand is reduced, compared to a strategy that fixes the indoor temperature, without compromising indoor comfort. Although this approach benefits the district heating system by reducing peak demand, housing companies may not adopt it unless there is a financial up-

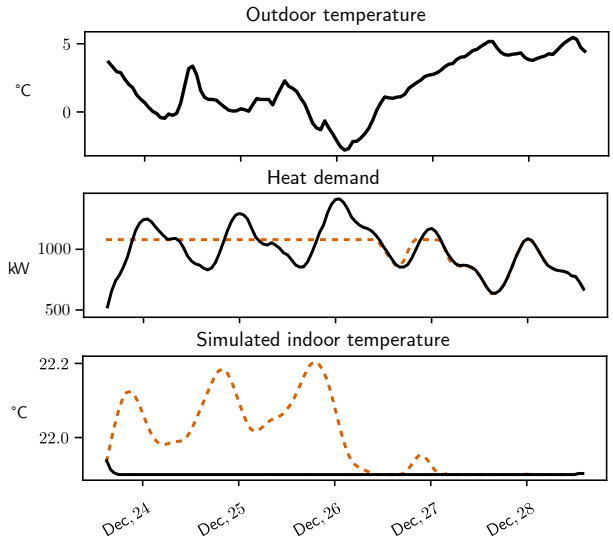

Figure 2.3: Load shifting Illustration of how load shifting reduces peak demand through temporary overheating. Based on a given outdoor air temperature profile, the figure shows indoor temperatures simulated for two control strategies: a conventional control strategy (black solid line) and a load shifting strategy (orange dashed line).

side to doing so. Most of the current price models primarily reflect long-term costs [20], but incorporating mechanisms to encourage short-term load shifting could improve both energy efficiency and the competitiveness of district heating compared to alternative heating sources, e.g., heat pumps.

Overheating

The Public Health Agency of Sweden recommends operators to aim for an indoor temperature between 20-23°C to stay within the acceptable range of 18-24°C [36]. Many apartments are substantially warmer than these recommended levels. An investigation in 2021 found that about 25% of Swedish apartments are warmer than 23°C [37]. This indicates that while comfort levels are generally high, such overheating means poor energy performance.

While the introduction of feedback controllers can mitigate overheating of

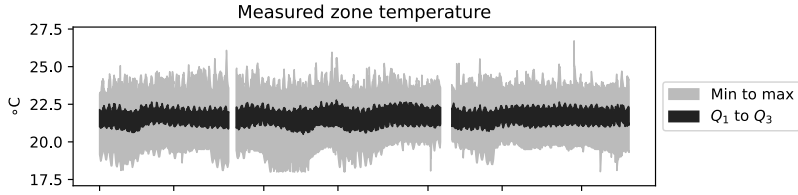

Figure 2.4: Zone temperature variation Measured zone temperatures of a Swedish heating system with 70 apartments during the winter 2023/2024. Q_1 to Q_3 denotes the first to third quartiles. The zone temperatures vary within an interval of 4°C, while the median temperature is around 22°C.

the average indoor temperature [19], significant temperature variation between thermal zones may persist due to improperly balanced radiator flow rates [38]. Figure 2.4 shows operational data from a Swedish heating system, in which some zones reach 25°C and others are simultaneously near the lower acceptable limit. By reducing the temperature variation, energy usage and costs can be reduced since fewer zones become overheated as a side effect.

2.3 Conventional Practice of Control and Configuration

The heating power output in a radiator depends on the flow rate and the supply temperature, and both are utilized in practice for controlling the heating power supply. The way they are used differs in control scope: flow rates can be adjusted individually for each radiator, while the supply temperature is uniform across the entire system. This section discusses current operational practices and highlights the remaining gaps that must be addressed to overcome the challenges outlined in Section 2.2.

Supply Temperature Control

Regulating the supply temperature is the primary method to regulate the radiators' heat output [18]. Traditionally, this is achieved using *weather compensation*, where the supply temperature is determined in open-loop as a function of the outdoor air temperature [39]. The principle of weather compensation

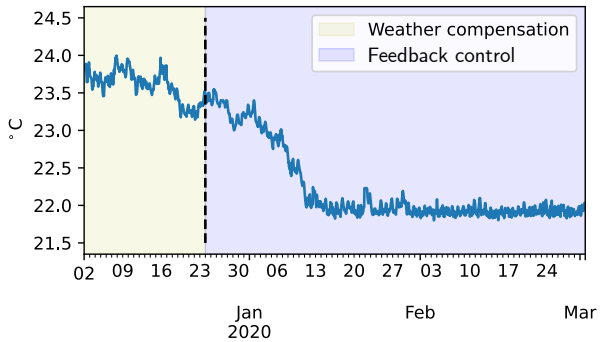

Figure 2.5: Feedback control Average zone temperature from a residential heating system showing how switching from pure weather compensation, with high and time-varying average temperature, to an extension including feedback control steadied the average temperature at a lower level.

is to correct the supply temperature for the thermal disturbance imposed by the weather conditions—colder outdoor temperatures lead to higher supply temperatures.

The traditional weather compensation setup lacks feedback from the indoor air temperature of the thermal zones, meaning that the supply temperature curve remains fixed regardless of whether zones are overheated or underheated. Research on utilizing feedback control in heating systems has grown significantly since the 2010s [40]. In Sweden, large-scale deployment of air temperature sensors has enabled feedback control to become an established practice for maintaining comfort in an energy-efficient manner [19]. Compared to traditional open-loop weather compensation, feedback control reduces the energy use by minimizing the overheating [41]. Figure 2.5 shows a successful example when weather compensation was extended with feedback control, which led to a steady average zone temperature and reduced overheating. However, it is important to note that this improvement primarily addresses the average temperature across zones. The variation in zone temperatures, as shown in Figure 2.4, is not resolved by this control shift.

Research on feedback control has mainly focused on model predictive control (MPC), typically formulated as optimizing the energy consumption while

maintaining constraints on the indoor climate, based on a predictive model of the system's heat dynamics [40]. While simpler controllers—such as Proportional-Integral (PI) control—can achieve similarly stable indoor temperatures without requiring a thermal model [42], the main advantage of MPC lies in its ability to optimize control actions with respect to an arbitrary cost function. This capability is relevant for demand-side management, where MPC can align the heat demand profile with the operational objectives of the district heating network. This includes the potential to control the indoor temperature in a time-varying manner, rather than being held constant [31], [43], as illustrated in Figure 2.3. Realizing this potential, however, depends on the availability of a cost function—the pricing mechanism—that accurately reflects the desired demand-side behavior.

Hydronic Balancing and Flow Rate Control

As reviewed in Section 2.1, radiator flow rates are governed by the statically configured balancing valves and the thermostatic radiator valves (TRVs). In the absence of any valves at all, radiators located closer to the substation—with shorter flow paths and lower hydraulic resistance—receive disproportionately high flow rates. Balancing valves are therefore installed to introduce additional resistance, ensuring a more equitable distribution of flow across all radiators [22].

In constant flow rate systems, radiator flows are entirely determined by the fixed settings of the balancing valves. However, even in variable flow rate systems—where TRVs dynamically adjust flows in response to heat demand—proper hydronic balancing remains essential. TRVs are not designed to handle significant under- or overflows, and without balanced baseline conditions, their control performance degrades significantly [30], [44].

The appropriate flow rate for a given radiator depends on both its heat output capacity and the thermal loss characteristics of the zone it serves. Conventionally, radiator flow rates are calculated using data from the construction plan, which characterizes the heat demand in each zone. Based on these calculations, each balancing valve is assigned a prescribed flow rate. However, because all valves are part of a hydraulically interconnected network, the configuration of each valve affects the pressure distribution—and thus the flow rates—throughout the entire system. Adjusting one riser valve, for instance, may unintentionally impact the flow in different risers. As a re-

sult, valve configurations must be coordinated and performed collectively to achieve system-wide balance [45].

The standard balancing procedure begins with measuring the valve flow rates when all balancing valves are fully open. Technicians then rank the valves by the ratio of measured to prescribed flow rates, starting with the lowest ratio, which usually corresponds to the path with the highest inherent resistance. Balancing proceeds pairwise: the first valve is matched with the second by gradually restricting the latter until their ratios align. The process continues sequentially (valve two with three, three with four, etc.) in an iterative, cascading manner until target flow rates are achieved throughout the network.

However, the prescribed flow rates often fail to immediately produce satisfactory indoor climate conditions, since the construction plan does not fully map to the real thermal conditions in the building. Consequently, a rebalancing phase is usually required, during which valve configurations are fine-tuned based on observed zone temperatures rather than prescribed flow rates. Because repeating the full balancing procedure is too labor-intensive, this phase usually involves small, localized reconfigurations, reducing flow to overheated zones and increasing flow to underheated ones.

Thus, balancing is a labor-intensive and time-consuming task, which has been cited as a key reason for the significant variation in zone temperatures often observed in practice [24]. In Sweden, some housing companies have even stopped performing full-system balancing at regular intervals, opting instead for incremental modifications in response to specific comfort issues [46]. Recent work has proposed improvements to the balancing procedure to reduce the number of required measurements [27], but these do not address the more fundamental issue—that prescribed flow rates based on construction data often fail to ensure satisfactory thermal comfort.

CHAPTER 3

Modeling of Thermal Dynamics

Thermal dynamics modeling can be classified into white-box, gray-box, and black-box approaches [47]. White- and gray-box models are based on physical principles and technical documentation, while gray- and black-box models rely on data-driven techniques. Gray-box models, which combine physical insight with data-based estimation, have gained popularity in recent literature.

This chapter provides a brief overview of modeling approaches, with an emphasis on reduced-order gray-box models. The structure is as follows: Section 3.1 presents the fundamentals of physical modeling for heating systems and the data requirements. Section 3.2 introduces a reduced-order gray-box model for a single thermal zone. Building on this, Section 3.3 extends the model to incorporate hydronic radiator behavior. Section 3.4 generalizes the approach to a multi-zone context. Finally, Section 3.5 outlines the procedure for estimating the model coefficients.

3.1 Physics-Based Modeling

The temperature dynamics in a building are primarily driven by two thermal processes: thermal leakage from the warm indoor air to the colder exterior,

and heating power supply from the warm water in the radiators. These processes are mediated by thermal masses such as the building envelope and radiator surfaces. A detailed representation of these dynamics is typically expressed by a system of linear differential equations—one for each heat transfer interaction (e.g., from indoor air to the inner wall surface), or through an equivalent RC-model [47].

To formulate these dynamics in a white-box manner requires comprehensive, up-to-date information about the building's physical characteristics, including its structure and materials. Although initiatives like Building Information Modeling (BIM) have been launched to maintain detailed information across the entire building lifecycle [48], older buildings often lack this level of documentation [49], [50]. In practice, the available documentation is non-digital and limited to original design or retrofit phases.

The lack of accurate technical documentation has, however, been mitigated by the collection of operational data, as enabled through increasing deployment of air temperature sensors, and the adoption of gray-box models–where coefficients of physical models are fitted to the operational data [47].

3.2 Reduced-Order Gray-Box Thermal Modeling

In a gray-box setting, the model selection is informed not only by physical principles but also by statistical considerations, such as the bias-variance tradeoff [51]. Although measurements of air temperatures are increasingly available, the temperatures of intermediate elements (e.g., walls or radiators) are not measured directly. Consequently, in a detailed modeling setup, such intermediate temperatures must be modeled as latent states, which effectively leads to second-order or higher-order dynamics and a larger number of parameters to estimate [52], [53]. Reduced gray-box models–where such intermediate states are omitted–can be advantageous as they reduce estimation variance.

The most reduced model that can be constructed in this manner is a first-order model. While this is a simplification of the underlying physics, it has nevertheless been shown to provide fair approximations [54], [55] and has proven useful for model-based control [56], [57]. For a single thermal zone, the most reduced form of a dynamic model that describes the aforementioned

thermal processes is the first-order system

$$\dot{y}(t) = \theta\ (w(t) - y(t)) + C\,\Phi(t) \tag{3.1}$$

where $y(t)$ is the indoor air temperature at time t, $\dot{y}(t)$ is its time derivative, C is a heat transfer coefficient, $\Phi(t)$ is the heating power output from the radiators, θ represents the thermal leakage through the building envelope, $w(t)$ is the outdoor temperature. In the formulation (3.1), other disturbances, e.g., internal heat gains driven by activity from the occupants, are omitted and will be discussed further in Section 3.5.

Although (3.1) is derived for a single thermal zone, it is often used as a lumped model of an entire building where y is the average temperature and Φ is the total heating power in the substation. Given measurements in the substation, the total heating power is given by

$$\Phi = q_{\text{tot}}\, c_p\, (u - r), \tag{3.2}$$

where q_{tot} is the flow rate in the heat exchanger at time t, c_p is the specific heat capacity of water, u is the supply temperature, and r is the return temperature.

3.3 Hydronic Radiators

Similar to the substation, the heating power output from a radiator is

$$\Phi = q_{\text{rad}}\, c_p\, (T_{\text{s}} - T_{\text{r}}), \tag{3.3}$$

where T_{s} is the radiator's supply temperature, T_{r} is its return temperature, and q is its flow rate. Unlike the substation, however, these quantities are typically not measured per radiator in real time. Nevertheless, in two-pipe systems, the radiator supply temperature T_{s} is approximately the substation supply temperature u [6], and flow rates q_{rad} are known and configured during hydronic balancing. While TRVs may modulate flow dynamically, the flow rate generally fluctuates around this nominal setting [22].

The return temperature T_{r} depends on q_{rad}, T_{s}, and the zone temperature y, and must therefore be modeled. Assuming a one-dimensional radiator of

length L, the energy balance at the position $x \in [0, L]$ gives

$$c_p q_{\text{rad}} \frac{dT}{dx} = h\,(y - T), \tag{3.4}$$

where h is a heat transfer coefficient and c_p is the specific heat capacity of water. Solving (3.4) with inlet condition $T(0) = T_{\text{s}} = u$ gives the return temperature

$$T_{\text{r}} = (u - y)\,\exp\left(\frac{-L\,h}{c_p\,q_{\text{rad}}}\right) + y. \tag{3.5}$$

The corresponding radiator heating power output becomes

$$\Phi = q_{\text{rad}}\,c_p\,\left(1 - \exp\left(\frac{-L\,h}{c_p\,q_{\text{rad}}}\right)\right)\,(u - y), \tag{3.6}$$

which is nonlinear in q_{rad} but linear in both u and y. Substituting this into the thermal dynamics in (3.1) gives

$$\dot{y}(t) = \theta\,(w(t) - y(t)) + \nu(q_{\text{rad}})\,(u(t) - y(t))\,, \tag{3.7}$$

where the lumped heating power coefficient is

$$\nu(q_{\text{rad}}) = C\,q_{\text{rad}}\,c_p\,\left(1 - \exp\left(\frac{-L\,h}{c_p\,q_{\text{rad}}}\right)\right). \tag{3.8}$$

Although not being the main focus in this work, there are approaches for more accurate modeling, such that the heat transfer coefficient h is treated as temperature-dependent

$$h \propto (y - T)^n, \tag{3.9}$$

where n is the *radiator exponent*, typically around 0.2 - 0.4 [58], [59]. This formulation leads to a nonlinear system that typically requires spatial discretization of the radiator and results in dynamics that are non-linear in the supply temperature T_{s}, which complicates analysis compared to the simplified form in (3.7).

3.4 Multi-Zone Formulation

As discussed in Section 3.2, single-zone models like (3.7) have frequently been used for modeling the average indoor climate. A single-zone model cannot capture temperature differences between zones, caused by improperly balanced radiator flow rates, since it lumps all zones together. To model zone-specific dynamics in a building with Z zones, the single-zone model in (3.7) is extended to the multi-zone system

$$\dot{\boldsymbol{y}}(t) = \operatorname{diag}(\boldsymbol{\theta})\,(\mathbb{1}w(t) - \boldsymbol{y}(t)) + \operatorname{diag}(\boldsymbol{\nu}(\boldsymbol{q}_{\mathrm{rad}}))\,(u(t) - \boldsymbol{y}(t)), \tag{3.10}$$

where $\boldsymbol{\theta}$, $\boldsymbol{\nu}(\boldsymbol{q}_{\mathrm{rad}}) \in \mathbb{R}^Z$, with $\boldsymbol{q}_{\mathrm{rad}} \in \mathbb{R}^Z$ being all radiator flow rates, are zone-wise leakage and heating power supply coefficients, i.e., each zone has its own coefficients. The inter-zone transfer is neglected in (3.10), which can be justified for the case during normal operation when all zone temperatures are within 20-25°C.

(3.10) highlights the two different ways of controlling the thermal dynamics: real-time control of the supply temperature T_{s} in the substation or balancing the flow rates $\boldsymbol{q}$, which will impact the heating power supply coefficients $\boldsymbol{\nu}(\boldsymbol{q})$, as given in (3.8).

3.5 Estimation of Thermal Coefficients

The coefficients $\boldsymbol{\theta}$ and $\boldsymbol{\nu}(\boldsymbol{q})$ in (3.10) can be estimated using measurements of $\boldsymbol{y}$, u, and w sampled at $t = 0, \Delta t, \ldots, N\Delta t$ by minimizing the mean squared error

$$\min \sum_{n=0}^{N-1} \left\| \hat{\boldsymbol{y}}(n\,\Delta t + \Delta t \mid n\,\Delta t) - \boldsymbol{y}(n\,\Delta t + \Delta t) \right\|^2 \tag{3.11}$$

where the one-step prediction is given by discretizing the continuous-time dynamics in (3.10) using the Euler forward method, giving

$$\begin{aligned} \hat{\boldsymbol{y}}(t + \Delta t \mid t) =& \boldsymbol{y}(t) + \Delta t \operatorname{diag}(\boldsymbol{\theta})\,(\mathbb{1}w(t) - \boldsymbol{y}(t)) \\ &+ \Delta t \operatorname{diag}(\boldsymbol{\nu}(\boldsymbol{q}))\,(\mathbb{1}u(t) - \boldsymbol{y}(t)) + \hat{\boldsymbol{v}}(t + \Delta t \mid t), \end{aligned} \tag{3.12}$$

where $\boldsymbol{v}(t)$ denotes an unmeasured disturbance, e.g., internal heat gains. If the disturbance $\boldsymbol{v}(t)$ is modeled as white, then

$$\hat{\boldsymbol{v}}(t + \Delta t \mid t) = \mathbf{0}. \tag{3.13}$$

However, in practice, especially during normal operation of heating systems, $\boldsymbol{v}(t)$ is not white [60]. In that case, one can introduce a parametrized model for $\boldsymbol{v}(t)$, such that also the color of the disturbance is estimated with the prediction error minimization in (3.11). However, as for the bias-variance tradeoff, the introduction of a disturbance model gives more parameters to estimate and, consequently, higher variance in those parameter estimates.

CHAPTER 4

System Optimization and Control

Building on the thermal modeling introduced in the previous Chapter 3, this chapter takes a mathematical approach to describe how the comfort and energy performance depends on the supply temperature control and hydronic balancing. In Section 4.1, the precision of control of the comfort is analyzed, illustrating how supply temperature control and hydronic balancing mechanisms influence the system's ability to track a reference indoor temperature. Section 4.2 provides a concise overview of the hydraulic principles underlying radiator flow rate adjustments via valve configurations. Finally, Section 4.3 discusses how supply temperature control can be formulated as Economic Model Predictive Control (MPC), offering a more practical representation of operational conditions and enabling better integration within a district heating network.

4.1 Precision of Comfort Control

Feedback from the thermal zone air temperatures enhances supply temperature control by mitigating temporal variations in the average indoor temperature. However, in a multi-zone system, the centrally controlled supply tem-

perature cannot alone compensate for temperature deviations in each zone individually. Therefore, achieving uniform comfort across all zones requires properly balanced flow rates, which eliminates temperature variation between zones. This section builds on the multi-zone thermal model introduced in Section 3.4, adopting a linear control framework to analyze how feedback and balancing jointly influence the precision of comfort control.

Error Dynamics

To analyze the control precision, we use the multi-zone thermal dynamics in (3.10), rearranged as

$$\dot{\boldsymbol{y}}(t) = -\mathrm{diag}(\boldsymbol{\theta} + \boldsymbol{\nu}(\boldsymbol{q}_{\mathrm{rad}}))\, \boldsymbol{y}(t) + \boldsymbol{\theta}\, w(t) + \boldsymbol{\nu}(\boldsymbol{q}_{\mathrm{rad}})\, u(t). \tag{4.1}$$

With the goal to maintain the reference temperature y_{ref} in every zone, the control error is defined as

$$\boldsymbol{e}(t) = \mathbb{1} y_{\mathrm{ref}} - \boldsymbol{y}(t). \tag{4.2}$$

Using the dynamics for a multi-zone system in (4.1), the error dynamics are

$$\begin{aligned}
\dot{\boldsymbol{e}}(t) &= \frac{d}{dt}(\mathbb{1}\, y_{\mathrm{ref}} - \boldsymbol{y}(t)) \\
&= -\,\dot{\boldsymbol{y}}(t) \\
&= \mathrm{diag}(\boldsymbol{\theta} + \boldsymbol{\nu}(\boldsymbol{q}_{\mathrm{rad}}))\, \boldsymbol{y}(t) - \boldsymbol{\theta}\, w(t) - \boldsymbol{\nu}(\boldsymbol{q}_{\mathrm{rad}})\, u(t) \\
&= \mathrm{diag}(\boldsymbol{\theta} + \boldsymbol{\nu}(\boldsymbol{q}_{\mathrm{rad}}))\, \boldsymbol{y}(t) - \boldsymbol{\theta}\, w(t) - \boldsymbol{\nu}(\boldsymbol{q}_{\mathrm{rad}})\, u(t) \\
&\quad + (\boldsymbol{\theta} + \boldsymbol{\nu}(\boldsymbol{q}_{\mathrm{rad}}))\, (y_{\mathrm{ref}} - y_{\mathrm{ref}}) \\
&= \underbrace{-\mathrm{diag}(\boldsymbol{\theta} + \boldsymbol{\nu}(\boldsymbol{q}_{\mathrm{rad}}))}_{\boldsymbol{A}}\, \boldsymbol{e}(t) + \boldsymbol{\theta}\, (y_{\mathrm{ref}} - w(t)) + \boldsymbol{\nu}(\boldsymbol{q}_{\mathrm{rad}})\, (y_{\mathrm{ref}} - u(t)).
\end{aligned} \tag{4.3}$$

From a control perspective, (4.3) represents a single-input multiple-output (SIMO) system with the supply temperature $u(t)$ as the input and the zone errors as the outputs. Since it is physically reasonable to assume $\mathbf{0} < \boldsymbol{\theta}$ and $\mathbf{0} < \boldsymbol{\nu}(\boldsymbol{q}_{\mathrm{rad}})$, the matrix $\boldsymbol{A}$ in (4.3) has strictly negative eigenvalues, i.e., the dynamics are inherently stable such that stabilization through control is not necessary. There are, however, disturbances acting on the system – the

weather and unmodeled disturbances such as internal heat gains – which are favorably rejected with the control mechanisms.

Weather Compensation and Impact from Balancing

Weather compensation is a feed-forward control strategy designed to reject the major disturbance—namely, the outdoor temperature—by utilizing real-time measurements. However, the effectiveness of this control approach depends on the system's balancing conditions. Under poor balancing, the effect of the outdoor temperature cannot be uniformly compensated across all zones, resulting in inter-zone temperature variation. With improved balancing conditions, the weather compensation can be configured with lower heat output and still ensure comfort in all zones.

The weather compensation control law is

$$u(t) = y_{\text{ref}} + F_w(y_{\text{ref}} - w(t)), \tag{4.4}$$

where F_w is the feed-forward gain for weather compensation. When substituting (4.4) into the error dynamics in (4.3), the resulting dynamics become

$$\begin{aligned}\dot{\boldsymbol{e}}(t) =& \boldsymbol{A}\,\boldsymbol{e}(t) + \boldsymbol{\theta}\,(y_{\text{ref}} - w(t)) \\ &+ \boldsymbol{\nu}(\boldsymbol{q}_{\text{rad}})\,(y_{\text{ref}} - y_{\text{ref}} - F_w\boldsymbol{\nu}(\boldsymbol{q}_{\text{rad}})(y_{\text{ref}} - w(t)) \\ =& \boldsymbol{A}\,\boldsymbol{e}(t) + \underbrace{(\boldsymbol{\theta} - F_w\,\boldsymbol{\nu}(\boldsymbol{q}_{\text{rad}}))\,(y_{\text{ref}} - w(t))}_{\boldsymbol{d}(t)}.\end{aligned} \tag{4.5}$$

This formulation demonstrates how the dynamics depend on the past error $\boldsymbol{e}(t)$ and the effective weather disturbance $\boldsymbol{d}(t)$. To minimize $\boldsymbol{d}(t)$, the optimal feedforward gain F_w is retrieved by minimizing the norm

$$F_w = \arg\min_{F_w} \|\boldsymbol{\theta} - \boldsymbol{\nu}(\boldsymbol{q}_{\text{rad}})\,F_w\|_2 = \frac{\boldsymbol{\theta}^\top \boldsymbol{\nu}(\boldsymbol{q}_{\text{rad}})}{\|\boldsymbol{\nu}(\boldsymbol{q}_{\text{rad}})\|^2}. \tag{4.6}$$

By substituting this optimal value of F_w into $\boldsymbol{d}(t)$, as given in (4.5), the remaining disturbance becomes

$$\boldsymbol{d}(t) = \left(\boldsymbol{\theta} - \frac{\boldsymbol{\theta}^\top \boldsymbol{\nu}(\boldsymbol{q}_{\text{rad}})}{\|\boldsymbol{\nu}(\boldsymbol{q}_{\text{rad}})\|^2}\boldsymbol{\nu}(\boldsymbol{q}_{\text{rad}})\right)(y_{\text{ref}} - w(t)). \tag{4.7}$$

Given this minimized weather disturbance, the inter-zone temperature variation will depend on the balancing conditions as manifested by the heat supply coefficient $\boldsymbol{\nu}(\boldsymbol{q}_{\text{rad}})$. To illustrate this, consider a two-zone system with $\boldsymbol{\theta} = \mathbb{1}$ and $\boldsymbol{\nu}(\boldsymbol{q}_{\text{rad}}) = \begin{bmatrix}0.9 & 1.1\end{bmatrix}^\top$ such that the effective disturbance becomes

$$\begin{aligned}\boldsymbol{d}(t) &= \left(\begin{bmatrix}1\\1\end{bmatrix} - \frac{0.9+1.1}{0.9^2+1.1^2}\begin{bmatrix}0.9\\1.1\end{bmatrix}\right)(y_{\text{ref}} - w(t)) \\ &= \left(\begin{bmatrix}1\\1\end{bmatrix} - 0.99\begin{bmatrix}0.9\\1.1\end{bmatrix}\right)(y_{\text{ref}} - w(t)) \\ &= \begin{bmatrix}0.1\\-0.1\end{bmatrix}(y_{\text{ref}} - w(t)),\end{aligned} \tag{4.8}$$

which means one zone experiences persistent overheating and the other persistent underheating. Because this disturbance is driven by the continuously acting outdoor temperature, the balancing conditions described by $\boldsymbol{\nu}(\boldsymbol{q}_{\text{rad}})$ results in a sustained temperature variation between zones.

By contrast, consider the case where $\boldsymbol{\nu}(\boldsymbol{q}_{\text{rad}}) = \begin{bmatrix}0.9 & 0.9\end{bmatrix}^\top$, i.e., parallel to $\boldsymbol{\theta} = \mathbb{1}$. The effective disturbance then becomes

$$\begin{aligned}\boldsymbol{d}(t) &= \left(\begin{bmatrix}1\\1\end{bmatrix} - \frac{0.9+0.9}{0.9^2+0.9^2}\begin{bmatrix}0.9\\0.9\end{bmatrix}\right)(y_{\text{ref}} - w(t)) \\ &= \left(\begin{bmatrix}1\\1\end{bmatrix} - 1.11\begin{bmatrix}0.9\\0.9\end{bmatrix}\right)(y_{\text{ref}} - w(t)) \\ &= \begin{bmatrix}0\\0\end{bmatrix},\end{aligned} \tag{4.9}$$

such that the disturbance is fully rejected in all zones through weather compensation. This highlights the importance of hydronic balancing: by configuring radiator flow rates $\boldsymbol{q}_{\text{rad}}$ such that the heat supply vector $\boldsymbol{\nu}(\boldsymbol{q}_{\text{rad}})$ is aligned with the thermal leakage vector $\boldsymbol{\theta}$, the disturbance can be minimized.

From an operational perspective, low temperature variation between zones, given from good balancing conditions, means that the reference y_{ref} in (4.4) can be set low while still maintaining thermal comfort in all zones. This is illustrated in Figure 4.1.

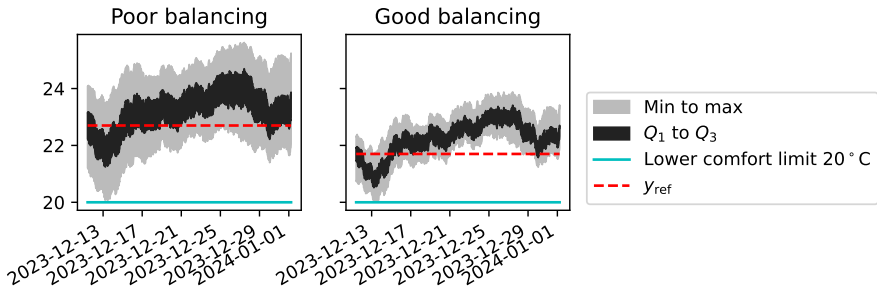

Figure 4.1: Balancing conditions Simulation demonstrating the benefit of good balancing conditions for weather compensation. With better balancing, the reference y_{ref} can be lowered while still ensuring that each zone temperature is above the lower limit at 20°C.

Feedback Control

Feedback control is enabled through the deployment of air temperature sensors. Unlike weather compensation, which targets only the outdoor temperature disturbance w, feedback control can, in addition to reduce the impact of outdoor temperature on the indoor air temperature, also reject other disturbances described by $\boldsymbol{v}$ in (3.12) but not modeled in (4.1). Such disturbances can include internal heat gains, human occupancy, and measurement noise.

The effect by deploying feedback control is that temporal variations in the zone temperatures are mitigated, such that they are, in general, closer to the reference temperature y_{ref}. However, just as with weather compensation, feedback control alone can not compensate for temperature variation across zones.

Adding a linear feedback term from the measured error $\boldsymbol{e}(t)$ to the weather compensation law in (4.4) gives

$$u(t) = y_{\text{ref}} - F_w(y_{\text{ref}} - w(t)) - \boldsymbol{F}_e^\top \boldsymbol{e}(t), \tag{4.10}$$

where $\boldsymbol{F}_e$ is the static feedback gain. The controllability matrix of the error dynamics in (4.3),

$$\left[\boldsymbol{A}\ \boldsymbol{A}\boldsymbol{\nu}(\boldsymbol{q}_{\text{rad}}) \dots \boldsymbol{A}^{Z-1}\boldsymbol{\nu}(\boldsymbol{q}_{\text{rad}})\right], \tag{4.11}$$

is of rank Z whenever $(\theta_i + \nu_i)\,\nu_i \neq (\theta_j + \nu_j)\,\nu_j$ for any pair of zones $i \neq j$

where $\boldsymbol{\nu}(\boldsymbol{q}_{\text{rad}}) = [\nu_1, \ldots, \nu_Z]^\top$. However, in practice, coefficients are often very similar between zones, i.e., $(\theta_i + \nu_i)\,\nu_i \approx (\theta_j + \nu_j)\,\nu_j$, and the rank is virtually always close to one. From a more practical perspective, there is only one control variable, the supply temperature u, which cannot compensate for poor balancing conditions but only for the average temperature error. This is illustrated with the following example of two zones and a feedback gain $\boldsymbol{F}_e^\top = \begin{bmatrix}1/2 & 1/2\end{bmatrix}$. For an observed error $\boldsymbol{e}(t_0) = \begin{bmatrix}1 & 1\end{bmatrix}^\top$ at time t_0, the control input becomes

$$\begin{aligned} u(t_0) &= y_{\text{ref}} - F_w(y_{\text{ref}} - w(t_0)) - \begin{bmatrix}1/2 & 1/2\end{bmatrix}\begin{bmatrix}1\\1\end{bmatrix} \\ &= y_{\text{ref}} - F_w(y_{\text{ref}} - w(t_0)) - 1, \end{aligned} \tag{4.12}$$

such that, compared with pure weather compensation without feedback, the feedback mechanism reduces the supply temperature $u(t_0)$ to mitigate uniform overheating across zones.

However, if the observed error is instead $\boldsymbol{e}(t_0) = \begin{bmatrix}1 & -1\end{bmatrix}^\top$ the control input is

$$\begin{aligned} u(t_0) &= y_{\text{ref}} - F_w(y_{\text{ref}} - w(t_0)) - \begin{bmatrix}1/2 & 1/2\end{bmatrix}\begin{bmatrix}1\\-1\end{bmatrix} \\ &= y_{\text{ref}} - F_w(y_{\text{ref}} - w(t_0)), \end{aligned} \tag{4.13}$$

which is identical to the pure weather-compensation case in (4.4). This illustrates that, in general, static feedback is effective when all zones are uniformly too hot or too cold—but cannot, in general, address simultaneous overheating in some zones and underheating in others.

Despite this limitation, feedback control improves the system's responsiveness to the unmodeled disturbances and reduces temporal fluctuations. As a result, the supply temperature reference y_{ref} can be lowered further than in the case of pure weather compensation, while still maintaining comfort. This is illustrated in Figure 4.2.

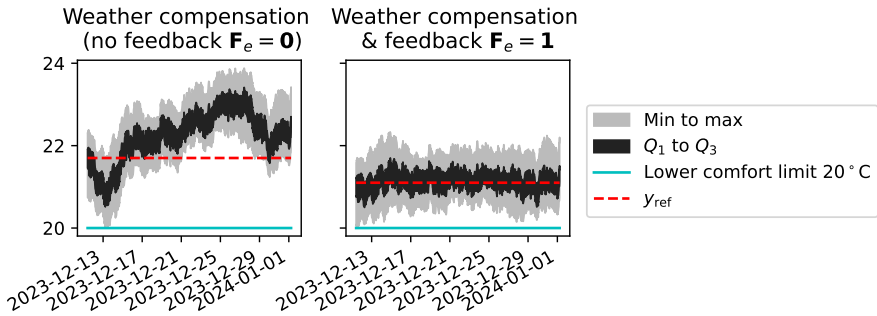

Figure 4.2: Feedback control Simulation demonstrating the benefit of employing feedback control. By reducing temporal variation, the reference y_{ref} can be lowered while still ensuring comfort. The left plot corresponds to the right-hand case in Figure 4.1.

4.2 Flow Rate Balancing

As discussed in Section 4.1, properly balanced radiator flow rates $\boldsymbol{q}_{\text{rad}}$ are essential to minimizing temperature variation across zones, a relationship governed by the heat supply coefficients $\boldsymbol{\nu}(\boldsymbol{q}_{\text{rad}})$. However, as noted in Section 2.3, achieving such balancing by manually adjusting valve settings is a challenging task. This is because all radiators are hydraulically connected, and the flow rates are mutually dependent across the system. In this section, we formalize the hydraulic model used to compute radiator flow rates as an implicit function of the valve configurations.

From a hydraulic standpoint, flow distribution is configured by adjusting valve resistances to compensate for fixed resistances in the piping and radiator network. The governing principles of the system are:

1. Mass conservation at each junction, meaning the total inflow equals the total outflow.

2. Pressure balance around each closed loop, meaning the net pressure drop is zero.

These principles are analogous to Kirchhoff's current and voltage laws for electrical circuits [61].

To illustrate this, consider the simple two-pipe system depicted in Fig-

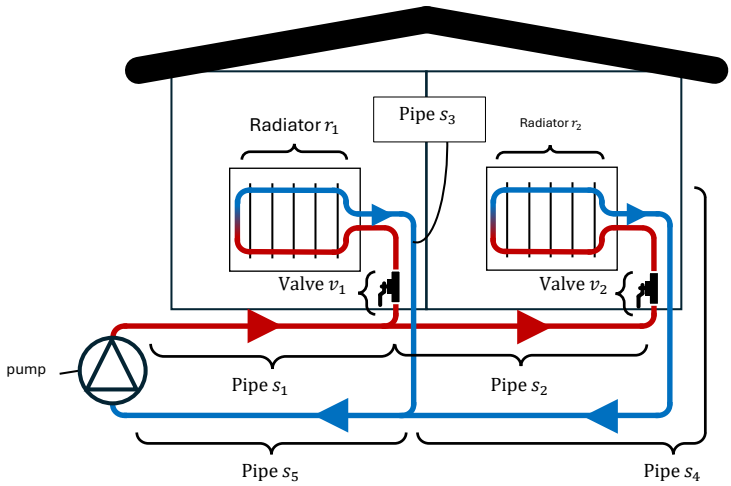

Figure 4.3: Example heating system Toy example of a simple two-pipe system with two radiators.

ure 4.3, which includes pipes s_1–s_5, valves v_1 and v_2, and radiators r_1 and r_2. The mass conservation principle yields the following flow rate equations:

$$\begin{cases} q_{s_1} = q_{v_1} + q_{s_2} \\ q_{v_1} = q_{r_1} \\ q_{r_1} = q_{s_3} \\ q_{s_2} = q_{v_2} \\ q_{v_2} = q_{r_2} \\ q_{r_2} = q_{s_4} \\ q_{s_3} + q_{s_4} = q_{s_5}. \end{cases} \tag{4.14}$$

The pressure balance principle gives:

$$\begin{cases} 0 = \Delta p_{\text{pump}} + \Delta p_{s_1} + \Delta p_{v_1} + \Delta p_{r_1} + \Delta p_{s_3} + \Delta p_{s_5} \\ 0 = \Delta p_{\text{pump}} + \Delta p_{s_1} + \Delta p_{s_2} + \Delta p_{v_2} + \Delta p_{r_2} + \Delta p_{s_4} + \Delta p_{s_5} \end{cases} \tag{4.15}$$
$$\Rightarrow$$
$$\Delta p_{v_1} + \Delta p_{r_1} + \Delta p_{s_3} = \Delta p_{s_2} + \Delta p_{v_2} + \Delta p_{r_2} + \Delta p_{s_4}$$

where the pump is assumed to provide a constant pressure increase Δp_{pump}.

Each pressure drop Δp is modeled as a quadratic function of flow rate q:

$$\Delta p = -k\, q^2, \tag{4.16}$$

where k is the hydraulic resistance. The resistance is fixed for pipes and radiators, but can be adjusted in valves via their opening positions.

For straight pipes, the resistance k is commonly calculated using the Darcy-Weisbach equation [6]:

$$k = \frac{8\,\rho\, l\, f}{\pi^2\, d^5}, \tag{4.17}$$

where ρ is the fluid density, l is the pipe length, d is the diameter, and f is the friction factor. The friction factor f depends on the Reynolds number and pipe roughness, and is often approximated using the Colebrook equation [6]:

$$\frac{1}{\sqrt{f}} = -2\,\log_{10}\left(\frac{2.51\,\pi\, d\,\mu}{4\,\rho\, q\,\sqrt{f}} + \frac{\varepsilon}{3.72\, d}\right), \tag{4.18}$$

which is valid across both laminar and turbulent flow regimes. Other empirical models with the same general form as (4.16) exist for specific components such as bends and T-junctions [22].

Taken together, (4.14), (4.15), (4.17) and (4.18) define a nonlinear system whose variables are the flow rates $q_{s_1}, \ldots, q_{s_5}$, q_{v_1}, q_{v_2}, q_{r_1}, and q_{r_2}, and the valve resistances k_{v_1} and k_{v_2}. Consequently, changing the valve setting for v_1 (i.e., modifying k_{v_1}) will not only affect the flow rate through radiator r_1, but also indirectly influence the flow through r_2 due to the interconnected nature of the hydraulic network.

4.3 Economic MPC

The controllers based on weather compensation in (4.4) and feedback in (4.10) are linear and primarily designed to minimize the control error $\boldsymbol{e}$ relative to the reference temperature y_{ref}. However, this objective does not fully capture operational priorities. In practice, housing companies seek to minimize heating costs while ensuring indoor comfort for residents. Framing supply temperature control as an optimization problem—with cost as the objective and comfort as constraints—better reflects these priorities. As will be shown later, this

perspective becomes increasingly advantageous under complex price models that are gaining importance in the evolving energy sector.

General MPC Formulation

Simplifying the thermal dynamics to a single-zone model, the supply temperature control can be formulated as an optimal control problem over the time horizon T:

$$\begin{aligned}
&\underset{u(t),\, y(t),\, \Phi(t),\, t \in [0,T]}{\text{minimize}} && J(\Phi) && \text{(4.19a)}\\
&\text{subject to} && y(0) = y_0 && \text{(4.19b)}\\
&&& \dot{y}(t) = \theta\,(w(t) - y(t)) + C\,\Phi(t) && \text{(4.19c)}\\
&&& \Phi(t) = \frac{\nu(q)}{C}\,(u(t) - y(t)) && \text{(4.19d)}\\
&&& L(t) \le y(t) \le U(t) && \text{(4.19e)}
\end{aligned}$$

Here, the objective function in (4.19a) represents the total heating cost over the control horizon based on the heating power output trajectory $\Phi(t)$. The constraint (4.19b) sets the initial indoor temperature. Equation (4.19c) describes the thermal dynamics of the building with a lumped single-zone model corresponding to (3.1). The heat output is computed using (4.19d), which corresponds to (3.6) and (3.8). The comfort constraint (4.19e) ensures that the indoor temperature remains within the allowable bounds $L(t)$ and $U(t)$.

Minimum Consumption Control

Traditionally, district heating price models have charged customers based solely on the heat energy consumed. This corresponds to the cost function

$$J(\Phi) = \int_0^T \Phi(t)dt \tag{4.20}$$

Under such a price model, the optimal control strategy is to maintain the indoor temperature as low as permitted by the comfort constraint (4.19e), which ultimately boils down to the linear controllers described in Section 4.1. Given such a linear controller that perfectly tracks a constant indoor temperature,

i.e., $\dot{y}(t) = 0$, the thermal dynamics in (4.19c) reduce to

$$\begin{aligned} 0 &= \dot{y}(t) \\ &\iff \\ 0 &= \theta\,(w(t) - y(t)) + C\,\Phi(t) \\ &\iff \\ \Phi(t) &= \frac{\theta}{C}\,(y(t) - w(t))). \end{aligned} \tag{4.21}$$

Thus, when the indoor temperature is constant, $\Phi(t)$ is smaller the lower the indoor temperature $y(t)$ is. Therefore, given (4.19) and (4.20) with a time-constant lower bound $L(t) = L$, the optimal indoor temperature equals the lower comfort bound $y(t) = L$. The supply temperature $u(t)$ obtained from such a formulation can be calculated by substituting the hydronic radiator approximation from (4.19d) into (4.21), yielding

$$\begin{aligned} \frac{\nu(q)}{C}(u(t) - y(t)) &= \frac{\theta}{C}\,(y(t) - w(t))) \\ &\iff \\ u(t) &= y(t) + \frac{\theta}{\nu(q)}(y(t) - w(t)) \\ &= y(t) + \frac{\nu(q)\,\theta}{\nu^2(q)}(y(t) - w(t)). \end{aligned} \tag{4.22}$$

This expression is of the same form as the weather compensation controller in (4.4). In other words, the optimal control policy resulting from the MPC formulation in (4.19) with the consumption objective in (4.20), given the initial temperature $y_0 = L$, coincides with the weather compensation controller in (4.4).

If instead the initial temperature satisfies $L < y_0 < U$, the optimal control trajectory resemble that of the feedback controller in (4.10), as it gradually reduces the indoor temperature toward the lower bound. If the initial temperature is too cold, $y_0 < L$, or too warm, $U < y_0$, the comfort constraint in (4.19e) becomes infeasible. In practice, this situation is typically handled by relaxing the comfort constraint.

Load Shifting through Minimum Peak Demand Control

Although the MPC formulation in (4.19) reduces to the linear controllers discussed in Section 4.1 under certain typical operating conditions, it is inherently more general. The objective function $L(\Phi)$ is not limited to minimizing total energy consumption, as in (4.20), but can incorporate arbitrary pricing schemes. For example, it can model time-varying heating costs—an increasingly popular approach in the control of heat pumps connected to electricity grids, where electricity prices vary hourly [62]. Moreover, the comfort constraint in (4.19e) can include time-varying temperature bounds $L(t)$ and $U(t)$. This is particularly relevant in buildings with intermittent occupancy, such as commercial or institutional facilities, where thermal comfort is only required during working hours.

While time-varying tariffs remain uncommon in district heating, utility providers have started to explore alternative price models, as the traditional consumption-based cost (4.20) does not accurately reflect the actual operational costs of district heating. In particular, production during peak load periods is significantly more expensive, as discussed in Section 2.2. To better align incentives with operational realities, price models often charge both the total energy consumption and the peak heating power, corresponding to

$$J(\Phi) = \lambda_{\text{con}} \int_0^T \Phi(t)\, dt + \lambda_{\text{peak}} \max_{t \in [0,T]} \Phi(t), \tag{4.23}$$

where λ_{con} is the energy price per kWh, and λ_{peak} denotes the price per kW of peak demand.

Under the cost function in (4.23), the optimal control strategy retrieved from (4.19) may differ significantly from the minimum consumption case. Specifically, the controller may permit some degree of overheating to reduce peak demand later. This strategy, known as load shifting, leverages the building's thermal inertia by preheating before the outdoor temperature drops, followed by a discharge phase during the cold peak. While load shifting effectively reduces the peak demand—thereby lowering the second term in (4.23)—it results in higher total energy use, since overheating increases thermal losses to the environment. Figure 4.4 illustrates this trade-off by comparing two control strategies: one that minimizes only energy consumption, corresponding to the cost function in (4.20), and one that minimizes only peak

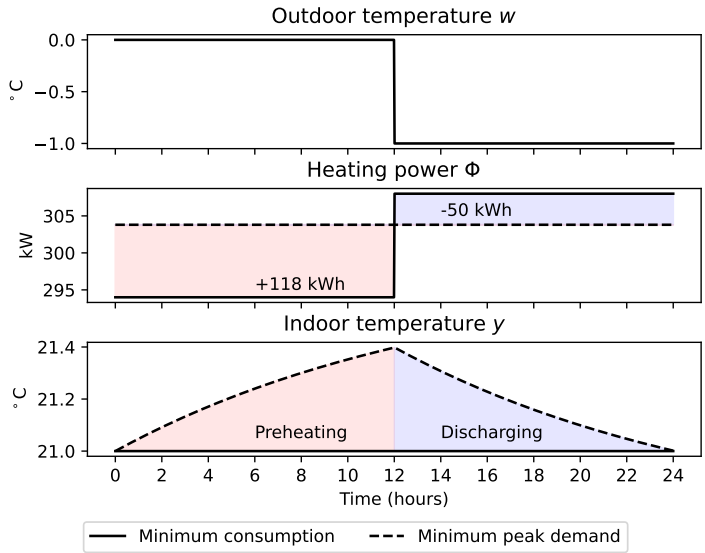

Figure 4.4: Consumption-peak demand tradeoff Illustration of load shifting under minimum peak demand control, compared to minimum consumption control. The outdoor temperature follows a negative step profile, and the lower comfort bound is set to $L = 21°\text{C}$. The minimum peak demand controller applies a preheating strategy to reduce heating power during the coldest period, resulting in an increased total heat energy use of 68 kWh (118 − 50 kWh).

demand, corresponding to (4.23) with zero energy cost weight $\lambda_{\text{con}} = 0$ and a nonzero peak demand cost $0 \leq \lambda_{\text{peak}}$. Due to the tradeoff between consumption and peak demand, the optimal extent of load shifting depends on the balance between the two cost components λ_{con} and λ_{peak}.

An important distinction should be made between the type of overheating discussed here and the overheating addressed in Section 4.1. In Section 4.1, overheating in certain zones is an undesired side effect of trying to prevent underheating elsewhere due to temperature variation across zones. In contrast, the formulation in this section is based on a lumped single-zone model, as given in (4.19), which does not capture spatial temperature variation within the building. Under this single-zone model, poor hydronic balancing—leading to significant temperature differences between zones—cannot be explicitly rep-

resented. Instead, such conditions necessitate conservative comfort margins: the lower bound $L(t)$ in (4.19e) may need to be set higher to ensure that no individual zone falls below the actual comfort threshold, which is even lower. Conversely, good balancing conditions allow for precise comfort control and may permit a higher degree of load shifting, as the upper bound $U(t)$ can be set high without risking uncomfortable overheating.

CHAPTER 5

Summary of Included Papers

This chapter provides a summary of the included papers.

5.1 Paper A

Henrik Håkanson, Magnus Önnheim, Emil Gustavsson, Mats Jirstrand
Effects on District Heating Networks by Introducing Demand-Side Economic Model Predictive Control
Published in Energy & Buildings,
vol. 309, no. 114051, Mar. 2024.

This paper investigates how different price models from district heating suppliers influence optimal demand-side control strategies in substation operation. The studied price models include two components: total energy consumption and weekly maximum heating power (peak demand), with varying relative cost weights. The demand-side control is formulated as an optimal control problem that minimizes heating costs while maintaining indoor temperatures within specified comfort bounds. Simulation results show that strong pe-

nalization of peak demand leads to control strategies that exploit the building's thermal inertia by allowing temporary overheating, resulting in slightly higher energy consumption. At the highest peak demand penalty, the peak can be reduced by 10% at the cost of only a 1% increase in total consumption compared to a baseline with no peak penalty. Additionally, the study explores time-varying comfort constraints and coordination across multiple substations. These strategies can achieve peak demand reductions of up to 20% with comparable energy consumption.

HH contributed with ideas, implementation, writing, results, and analysis. MÖ and EG contributed to the idea generation, implementation, analysis, and writing. MJ contributed to writing.

5.2 Paper B

Henrik Håkanson, Magnus Önnheim, Jonas Sjöberg, Mats Jirstrand
Model-Assisted Hydronic Balancing in Residential Heating Systems using Operational Sensor Data
Accepted in *Energy & Buildings*, June 2025 .

This paper explores methods for leveraging modeling and operational data to improve hydronic balancing and ultimately reduce temperature variation between thermal zones. A method for evaluating the performance of the radiator flow rates is suggested that is based on parameters of a model for the thermal dynamics in all zones. The proposed evaluation method is demonstrated using data collected during a rebalancing event, where radiator flow rates were adjusted by reconfiguring valves. By identifying model parameters before and after rebalancing, the method indicates improved balancing conditions, which correspond to a measurable reduction in temperature variance. Furthermore, methods for calculating valve reconfigurations are developed through hydraulic modeling of the pipe network. Applying this method to pre-rebalancing data successfully predicts that the implemented rebalancing would enhance balancing conditions. Additionally, the method suggests alternative rebalancing strategies that could potentially yield even greater improvements.

HH contributed with ideas, implementation, writing, results, and analysis. MÖ, JS, and MJ contributed to the idea generation and writing.

CHAPTER 6

Concluding Remarks and Future Work

This thesis has presented insights and methods aimed at enabling energy-efficient operation of hydronic heating systems while maintaining occupant comfort. A central focus of the work has been to ensure that the proposed methods are suitable for real-world implementation by relying solely on equipment already installed in many buildings.

One of the two main contributions of the thesis are insights in the design of district heating price models to incentivize load shifting. The simulation study presented in Paper A demonstrates that, by appropriately weighting tariffs, it is possible to provide housing companies with financial incentives to reduce peak demand. The second major contribution lies in the data-driven modeling of radiator flow balancing, which aims to simplify the balancing procedure. Paper B introduces a weather-independent evaluation method and an optimization framework for determining suitable valve adjustments, both of which are demonstrated using real operational data.

To summarize, the results from this thesis shows that, by adopting the modeling techniques and utilizing the data already available from the existing systems, the energy performance of hydronic heating systems can be improved without compromising occupant comfort.

6.1 Future Work

This thesis has focused on solutions compatible with currently installed equipment, but significant potential remains in exploring the use of emerging equipment technologies. One example would be connected TRVs at each radiator, which enable more precise monitoring and control. A direction for future research would be to conduct a cost-benefit analysis to compare the added capabilities of such equipment with its financial and operational implications.

Another area for further exploration is system identification using operational data. When collecting data under normal conditions, the ability to excite the system is limited, as occupant comfort is always prioritized, and system identification becomes challenging. Future work could investigate how to combine these competing objectives by designing control input signals or operational strategies that ensure acceptable comfort levels while simultaneously improving the data quality needed for effective system identification.

Finally, this work has primarily adopted the perspective of the housing company—focusing on district heating price models and hydronic balancing—but there are broader system interactions. For instance, coupling the price model with a district heating plant model could provide insight into the true operational costs and benefits for the energy utility. Additionally, while improved hydronic balancing can reduce costs for housing companies, it may also enhance the system's capacity for load shifting. Understanding the value this creates for the district heating provider would open up new opportunities for collaboration and optimization across the entire energy supply chain.

References

[1] European Parliament and Council of the European Union, "Regulation (EU) 2021/1119 of the European Parliament and of the Council of 30 June 2021 establishing the framework for achieving climate neutrality and amending Regulations (EC) No 401/2009 and (EU) 2018/1999 ('European Climate Law')," *Official Journal of the European Union*, L, Jun. 2021, Legislative Body: CONSIL, EP.

[2] Council of the European Union, "Council Regulation (EU) 2022/1369 of 5 August 2022 on coordinated demand-reduction measures for gas," *Official Journal of the European Union*, L, Aug. 2022, Legislative Body: CONSIL.

[3] Council of the European Union and European Parliament, "Directive (EU) 2023/1791 of the European Parliament and of the Council of 13 September 2023 on energy efficiency and amending Regulation (EU) 2023/955," *Official Journal of the European Union*, L, Sep. 2023.

[4] O. Ruhnau, C. Stiewe, J. Muessel, and L. Hirth, "Natural gas savings in Germany during the 2022 energy crisis," en, *Nature Energy*, vol. 8, no. 6, pp. 621–628, May 2023, ISSN: 2058-7546.

[5] E. Meza, "80 percent of German households lowered heating this winter – report," *Clean Energy Wire*, Jan. 2023.

[6] American Society of Heating, Refrigerating and Air-Conditioning Engineers, Inc., *2024 ASHRAE Handbook - Heating; Ventilating; and Air-Conditioning Systems and Equipment (SI Edition)*. American Society of

Heating, Refrigerating and Air-Conditioning Engineers, Inc. (ASHRAE), 2024, ISBN: 978-1-955516-84-6.

[7] "The Future of Heat Pumps," International Energy Agency, Paris, Tech. Rep., Nov. 2022.

[8] P. P. Altermatt, J. Clausen, H. Brendel, *et al.*, "Replacing gas boilers with heat pumps is the fastest way to cut German gas consumption," en, *Communications Earth & Environment*, vol. 4, no. 1, pp. 1–8, Mar. 2023, Publisher: Nature Publishing Group, ISSN: 2662-4435.

[9] H. Lund, B. Möller, B. V. Mathiesen, and A. Dyrelund, "The role of district heating in future renewable energy systems," *Energy*, vol. 35, no. 3, pp. 1381–1390, Mar. 2010, ISSN: 0360-5442.

[10] S. Werner, "International review of district heating and cooling," *Energy*, vol. 137, pp. 617–631, Oct. 2017, ISSN: 0360-5442.

[11] N. Martin, J. Zinck Thellufsen, M. Chang, L. Talens-Peiró, and C. Madrid-López, "The many faces of heating transitions. Deeper understandings of future systems in Sweden and beyond," *Energy*, vol. 290, no. 130264, Mar. 2024, ISSN: 0360-5442.

[12] D. Connolly, H. Lund, B. V. Mathiesen, *et al.*, "Heat Roadmap Europe: Combining district heating with heat savings to decarbonise the EU energy system," *Energy Policy*, vol. 65, pp. 475–489, Feb. 2014, ISSN: 0301-4215.

[13] D. Lander, Y. Selander, H. Jennehov, *et al.*, "Analys av fjärrvärmemarknaden - Konsultrapport Sweco," The Swedish Energy Markets Inspectorate, Tech. Rep., Aug. 2023.

[14] C. Hjortling, F. Björk, M. Berg, and T. a. Klintberg, "Energy mapping of existing building stock in Sweden – Analysis of data from Energy Performance Certificates," *Energy and Buildings*, vol. 153, pp. 341–355, Oct. 2017, ISSN: 0378-7788.

[15] M. Mangold, M. Österbring, and H. Wallbaum, "A review of Swedish residential building stock research," *International Journal of Environmental Sustainability*, vol. 11, no. 2, 2015.

[16] É. Mata, A. Sasic Kalagasidis, and F. Johnsson, "Energy usage and technical potential for energy saving measures in the Swedish residential building stock," *Energy Policy*, Special section: Long Run Transitions to Sustainable Economic Structures in the European Union and Beyond, vol. 55, pp. 404–414, Apr. 2013, ISSN: 0301-4215.

[17] S. Frederiksen and S. Werner, *District Heating and Cooling*, 1st ed. Lund University, Lund, Sweden, 2013, ISBN: 978-91-44-08530-2.

[18] M. Dahlblom, B. Nordquist, and L. Jensen, "Evaluation of a feedback control method for hydronic heating systems based on indoor temperature measurements," *Energy and Buildings*, vol. 166, pp. 23–34, May 2018, ISSN: 0378-7788.

[19] D. Olsson, P. Filipsson, and A. Trüschel, "Feedback Control in Swedish Multi-Family Buildings for Lower Energy Demand and Assured Indoor Temperature—Measurements and Interviews," en, *Energies*, vol. 16, no. 18-6747, Jan. 2023, Number: 18 Publisher: Multidisciplinary Digital Publishing Institute, ISSN: 1996-1073.

[20] J. Song, F. Wallin, H. Li, and B. Karlsson, "Price Models of District Heating in Sweden," *Energy Procedia*, CUE 2015 - Applied Energy Symposium and Summit 2015: Low carbon cities and urban energy systems, vol. 88, pp. 100–105, Jun. 2016, ISSN: 1876-6102.

[21] A. Vandermeulen, B. van der Heijde, and L. Helsen, "Controlling district heating and cooling networks to unlock flexibility: A review," *Energy*, vol. 151, pp. 103–115, May 2018, ISSN: 0360-5442.

[22] A. Trüschel, *Hydronic Heating Systems The Effect of Design on System Sensitivity*, en. 2002, ISBN: 978-91-7291-175-8.

[23] L. Zhang, J. Xia, J. E. Thorsen, O. Gudmundsson, H. Li, and S. Svendsen, "Method for achieving hydraulic balance in typical Chinese building heating systems by managing differential pressure and flow," en, *Building Simulation*, vol. 10, no. 1, pp. 51–63, Feb. 2017, ISSN: 1996-8744.

[24] H. Averfalk and S. Werner, "Essential improvements in future district heating systems," *Energy Procedia*, 15th International Symposium on District Heating and Cooling, DHC15-2016, 4-7 September 2016, Seoul, South Korea, vol. 116, pp. 217–225, Jun. 2017, ISSN: 1876-6102.

[25] K. Lygnerud, T. Nyberg, A. Nilsson, *et al.*, "A study on how efficient measures for secondary district heating system performance can be encouraged by motivational tariffs," en, *Energy, Sustainability and Society*, vol. 13, no. 38, Oct. 2023, ISSN: 2192-0567.

[26] R. E. Hedegaard, M. H. Kristensen, T. H. Pedersen, A. Brun, and S. Petersen, "Bottom-up modelling methodology for urban-scale analysis of residential space heating demand response," *Applied Energy*, vol. 242, pp. 181–204, May 2019, ISSN: 0306-2619.

[27] F. Pedranzini, L. P. M. Colombo, and F. Romano, "Development and Application of a Novel Non-Iterative Balancing Method for Hydronic Systems," en, *Applied Sciences*, vol. 14, no. 6232, Jan. 2024, Number: 14 Publisher: Multidisciplinary Digital Publishing Institute, ISSN: 2076-3417.

[28] E. A. Piana, B. Grassi, F. Bianchi, and C. Pedrotti, "Hydraulic balancing strategies: A case study of radiator-based central heating system," EN, *Building Services Engineering Research & Technology*, vol. 39, no. 3, pp. 249–262, May 2018, Publisher: SAGE Publications Ltd STM, ISSN: 0143-6244.

[29] T. Cholewa, I. Balen, and A. Siuta-Olcha, "On the influence of local and zonal hydraulic balancing of heating system on energy savings in existing buildings – Long term experimental research," *Energy and Buildings*, vol. 179, pp. 156–164, Nov. 2018, ISSN: 0378-7788.

[30] F. Tahersima, J. Stoustrup, and H. Rasmussen, "An analytical solution for stability-performance dilemma of hydronic radiators," *Energy and Buildings*, vol. 64, pp. 439–446, Sep. 2013, ISSN: 0378-7788.

[31] C. A. Thilker, P. Bacher, and H. Madsen, "Learnings from experiments with MPC for heating of older school building," en, *E3S Web of Conferences*, vol. 362, no. 12004, 2022, Publisher: EDP Sciences, ISSN: 2267-1242.

[32] V. Edenhofer and D. Olsson, "Elektroniska termostater i flerbostadshus," Swedish, Bebostad, Prestudy 2023:08, Feb. 2024.

[33] J. Kensby, A. Trüschel, and J.-O. Dalenbäck, "Potential of residential buildings as thermal energy storage in district heating systems – Results from a pilot test," *Applied Energy*, vol. 137, pp. 773–781, Jan. 2015, ISSN: 0306-2619.

[34] J. Le Dréau and P. Heiselberg, "Energy flexibility of residential buildings using short term heat storage in the thermal mass," *Energy*, vol. 111, pp. 991–1002, Sep. 2016, ISSN: 0360-5442.

[35] D. F. Dominković, P. Gianniou, M. Münster, A. Heller, and C. Rode, "Utilizing thermal building mass for storage in district heating systems: Combined building level simulations and system level optimization," *Energy*, vol. 153, pp. 949–966, Jun. 2018, ISSN: 0360-5442.

[36] Folkhälsomyndigheten, *Tillsynsvägledning om temperatur inomhus*, sv, May 2024.

[37] D. Teli, T. Psomas, S. Langer, A. Trüschel, and J.-O. Dalenbäck, "Drivers of winter indoor temperatures in Swedish dwellings: Investigating the tails of the distribution," *Building and Environment*, vol. 202, no. 108018, Sep. 2021, ISSN: 0360-1323.

[38] H.-I. Cho, D. Cabrera, and M. K. Patel, "Estimation of energy savings potential through hydraulic balancing of heating systems in buildings," *Journal of Building Engineering*, vol. 28, no. 101030, Mar. 2020, ISSN: 2352-7102.

[39] S. Prívara, J. Široký, L. Ferkl, and J. Cigler, "Model predictive control of a building heating system: The first experience," *Energy and Buildings*, vol. 43, no. 2, pp. 564–572, Feb. 2011, ISSN: 0378-7788.

[40] J. Drgoňa, J. Arroyo, I. Cupeiro Figueroa, *et al.*, "All you need to know about model predictive control for buildings," *Annual Reviews in Control*, vol. 50, pp. 190–232, Jan. 2020, ISSN: 1367-5788.

[41] H. T. Walnum, I. Sartori, P. Ward, and S. Gros, "Demonstration of a low-cost solution for implementing MPC in commercial buildings with legacy equipment," *Applied Energy*, vol. 380, no. 125012, Feb. 2025, ISSN: 0306-2619.

[42] D. Olsson, P. Filipsson, and A. Trüschel, "Weather Forecast Control for Heating of Multi-Family Buildings in Comparison with Feedback and Feedforward Control," en, *Energies*, vol. 17, no. 261, Jan. 2024, Number: 1 Publisher: Multidisciplinary Digital Publishing Institute, ISSN: 1996-1073.

[43] H. T. Walnum, I. Sartori, and M. Bagle, *Model predictive control of District Heating substations for flexible heating of buildings*, eng. SINTEF Academic Press, 2020, Accepted: 2020-10-16T07:13:21Z ISSN: 2387-4295 Publication Title: 123-130, ISBN: 978-82-536-1679-7.

[44] D. S. Østergaard and S. Svendsen, "Experience from a practical test of low-temperature district heating for space heating in five Danish single-family houses from the 1930s," *Energy*, vol. 159, pp. 569–578, Sep. 2018, ISSN: 0360-5442.

[45] R. Petitjean, *Balancing of distribution systems*, 2nd. Tour & Andersson Hydronics AB, 2000.

[46] D. Olsson, "Behovsanpassad värmereglering," Bebostad, Prestudy 2022:052, Aug. 2022.

[47] Z. Afroz, G. Shafiullah, T. Urmee, and G. Higgins, "Modeling techniques used in building HVAC control systems: A review," *Renewable and Sustainable Energy Reviews*, vol. 83, pp. 64–84, Mar. 2018, ISSN: 1364-0321.

[48] H. Gao, C. Koch, and Y. Wu, "Building information modelling based building energy modelling: A review," *Applied Energy*, vol. 238, pp. 320–343, Mar. 2019, ISSN: 0306-2619.

[49] A. Gökgür, "Current and future use of BIM in renovation projects," eng, 2015.

[50] S. Durdyev, G. Dehdasht, S. R. Mohandes, and D. J. Edwards, "Review of the Building Information Modelling (BIM) Implementation in the Context of Building Energy Assessment," *Energies*, vol. 14, no. 24-8487, Jan. 2021, Number: 24 Publisher: Multidisciplinary Digital Publishing Institute, ISSN: 1996-1073.

[51] T. Hastie, R. Tibshirani, J. Friedman, *et al.*, *The elements of statistical learning*, 2009.

[52] P. Bacher and H. Madsen, "Identifying suitable models for the heat dynamics of buildings," *Energy and Buildings*, vol. 43, no. 7, pp. 1511–1522, Jul. 2011, ISSN: 0378-7788.

[53] C. A. Thilker, P. Bacher, H. G. Bergsteinsson, R. G. Junker, D. Cali, and H. Madsen, "Non-linear grey-box modelling for heat dynamics of buildings," *Energy and Buildings*, vol. 252, no. 111457, Dec. 2021, ISSN: 0378-7788.

[54] H. Harb, N. Boyanov, L. Hernandez, R. Streblow, and D. Müller, "Development and validation of grey-box models for forecasting the thermal response of occupied buildings," *Energy and Buildings*, vol. 117, pp. 199–207, Apr. 2016, ISSN: 0378-7788.

[55] R. Serasinghe, N. Long, and J. D. Clark, "Parameter identification methods for low-order gray box building energy models: A critical review," *Energy and Buildings*, vol. 311, no. 114123, May 2024, ISSN: 0378-7788.

[56] S. Prívara, J. Cigler, Z. Váňa, F. Oldewurtel, C. Sagerschnig, and E. Žáčeková, "Building modeling as a crucial part for building predictive control," *Energy and Buildings*, vol. 56, pp. 8–22, Jan. 2013, ISSN: 0378-7788.

[57] S. F. Fux, A. Ashouri, M. J. Benz, and L. Guzzella, "EKF based self-adaptive thermal model for a passive house," *Energy and Buildings*, vol. 68, pp. 811–817, Jan. 2014, ISSN: 0378-7788.

[58] T. H. Pedersen, R. E. Hedegaard, K. F. Kristensen, B. Gadgaard, and S. Petersen, "The effect of including hydronic radiator dynamics in model predictive control of space heating," en, *Energy and Buildings*, vol. 183, pp. 772–784, Jan. 2019, ISSN: 0378-7788.

[59] L. H. Hansen, *Stochastic modelling of central heating systems* (IMM-PHD-1997-34). Kgs. Lyngby: Technical University of Denmark, 1997.

[60] L. Ferkl and Jan Široký, "Ceiling radiant cooling: Comparison of ARMAX and subspace identification modelling methods," *Building and Environment*, International Symposium on the Interaction between Human and Building Environment Special Issue Section, vol. 45, no. 1, pp. 205–212, Jan. 2010, ISSN: 0360-1323.

[61] L. Ljung and T. Glad, *Modellbygge och simulering*. Studentlitteratur, 1991.

[62] R. Halvgaard, N. K. Poulsen, H. Madsen, and J. B. Jørgensen, "Economic Model Predictive Control for building climate control in a Smart Grid," in *2012 IEEE PES Innovative Smart Grid Technologies (ISGT)*, Jan. 2012, pp. 1–6.

[63] H. Håkansson, M. Önnheim, E. Gustavsson, and M. Jirstrand, "Effects on district heating networks by introducing demand side economic model predictive control," *Energy and Buildings*, vol. 309, no. 114051, Apr. 2024, ISSN: 0378-7788.